A PANEL METHOD BASED AERODYNAMIC CODE FOR ANALYSIS OF WIND TURBINE BLADES

Santiago Martin Lugones [a], s_lugones@hotmail.com
Mauricio Vicente Donadon [a], donadon@ita.br
Ana Scarabino [b], scarabino@ing.unlp.edu.ar

Instituto Tecnológico de Aeronáutica [a], CTA-ITA-IEM, Pça Mal. Eduardo Gomes n[0] 50, 12228-900, São José dos Campos, SP, Brazil

Universidad Nacional de La Plata [b], LACLyFA; Calle 116 e/47 y 48, CP 1900, La Plata, BsAs, Argentina.

Abstract*. The size of commercial wind turbines has increased dramatically in the last 25 years from approximately a rated power of 50kW and a rotor diameter of 10–15m up to today's commercially available 5MW machines with a rotor diameter of more than 120 m. This development has forced the development of reliable numerical tools which enable the prediction of steady and unsteady aerodynamic loads not only in the wind turbine blades but also in the entire wind turbine construction, including tower, drive train, rotor and control system.*
Within this context, this paper presents a steady-state panel method formulation based code for aerodynamic load prediction in wind turbine blades. The formulation is fully three-dimensional accounting for wake and rotational angular speed effects. A 2MW wind turbine blade has been taken as a study case to demonstrate the code capabilities.

Keywords*: Wind turbines, aerodynamics blade design, 3D panel method, source doublet*

1   INTRODUCTION

Since the demand for energy, more specifically electricity, has increased dramatically over the last 100 years, it has now become important to consider the environmental impacts of energy production. An increase reliance on the energy from the wind for instance, will decrease the chance of environmental impacts such as global warming, since this renewable energy resource does not emit greenhouse gasses and obviously produce no nuclear waste compared to most conventional sources of energy. Within this context, this paper focuses on the development of a blade design tool for horizontal axis wind turbines with variable geometry. The design tool consists of an in-house MATLAB program based on the Glauert Blade Element Theory, including blade pitching and blade twisting effects. The program enables predictions of aerodynamic power and forces acting on the wind turbine blades for a given operating condition. Numerical results in terms of aerodynamic performance are presented for a 2 MW wind turbine.

The aerodynamic model for the wind turbine blades presented in this work is based on the Glauert Blade Element Theory. In this method the blade is divided into a number of independent sections along the length. At each section a force balance is applied involving 2D section lift and drag. At the same time a balance of axial and angular momentum is applied. This produces a set of non-linear equations that can be solved by iteration for each blade section. This theory does not include secondary effects such as 3-D flow velocities power and forces. Therefore, this work is going to present the Doublet Lattice Method to generate them for a wind turbine blade.

The purpose of most wind turbine is extracting the most quantity of energy from wind. Therefore, each component of this turbine should be optimized for that purpose.

It's usual to consider that the turbine induces a velocity variation to the free stream velocity. The stream-wise induced component will be defined as $-aU_\infty$ and for now on, a will be known as the **'axial flow induction factor'** or inflow factor.

The flow entering the actuator disc has no rotational motion at all. The flow exiting the disc does have rotation and that rotation remains constant as the fluid progresses down the wake. The transfer of rotational motion to the air takes place entirely across the thickness of the disc (see Figure 1.1). The change in tangential velocity is expressed in terms of a **tangential flow induction factor (a')**.
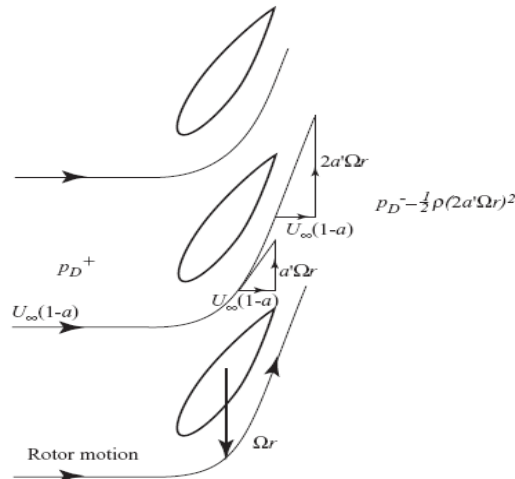

Figure 1.1. *Tangential Velocity Grows Across the Disc Thickness [1]*

All of the data generated with the 'blade element theory' will be used as the input data to the numerical construction based on the panels method.

The application of numerical techniques allows the treatment of more realistic geometries when compare with the analytical techniques. The doublet lattice method description presented here is based on the surface distribution of singularity elements, which is a logical extension of the analytical method found in the open literature. Since the solution is to reduce finding the strength of the singularity elements distributed along the body's surface. This approach seems to be more economical, from the computational point of view, than the method that solve for the flowfield in the whole fluid volume (e.g., finite-difference method). Of course this comparison holds for inviscid incompressible flows only, whereas numerical methods such as finite-differences were basically developed to solve more complex flowfields where compressibility and viscous effects are not negligible.

2   BLADE ELEMENT THEORY

It is assumed that the forces on a blade element can be calculated by means of two-dimensional aerofoil characteristics using an angle of attack determined from the incident resultant velocity in the cross-sectional plane of the element; the velocity component in the span-wise direction is ignored. Three-dimensional effects are also ignored.

The velocity components at a radial position of the blade expressed in terms of the wind speed, the flow factors and the rotational speed of the rotor will determine the angle of attack. Having information about how the aerofoil characteristic coefficients C_l and C_d vary with the angle of attack the forces on the blades for given values of a and a'. can be determined.

Consider a turbine with N blades of tip radius R each with chord c and set pitch angle β measured between the *aerofoil zero lift line* and the plane of the disc. Both the chord length and the pitch angle may vary along the blade span. Let the blades be rotating at angular velocity Ω and let the wind speed be U_∞. The tangential velocity (Ωr) of the blade element shown in Figure 2.1 combined with the tangential velocity of the wake ($a'\Omega r$) means that the net tangential flow

velocity experienced by the blade element is $(1 + a')\Omega r$. Figure 2.2 shows all the velocities and forces relative to the blade chord line at radius r.
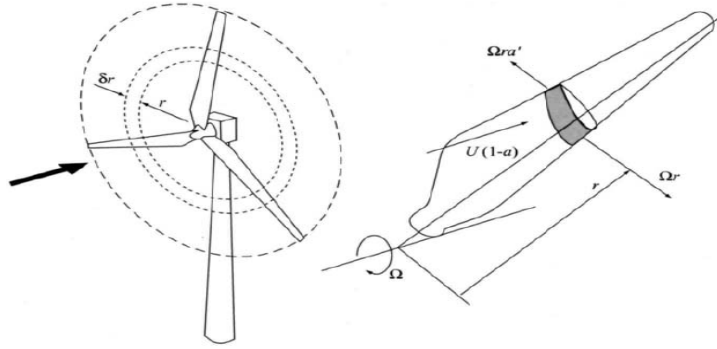

Figure 2.1. *A blade element sweep out an angular ring [1]*

From Figure 2.2 the resultant relative velocity at the blade is,

$$W = \sqrt{U_\infty{}^2(1-a)^2 + \Omega^2 r^2 (1+a')^2}$$

2.1

This equation will provide the velocity magnitude input data to the doublet lattice method (Figure 2.3)

The resultant relative velocity (W) acts at an induction flow angle ϕ to the plane of rotation (used as an input data too), such that,

$$sin\phi = \frac{U_\infty(1-a)}{W} \text{ e } cos\phi = \frac{\Omega r(1+a')}{W}$$

2.2

The angle of attack α (being β the pitch angle) is then given by:

$$\alpha = \phi - \beta$$
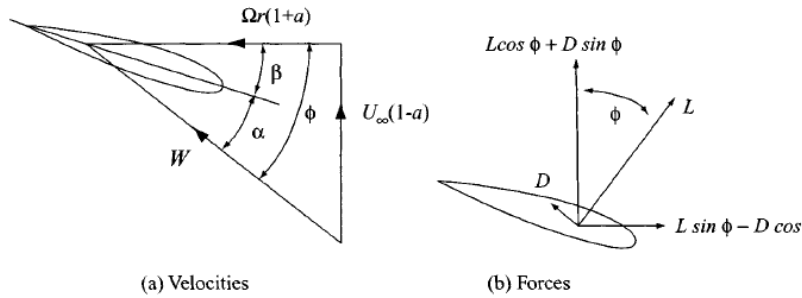
2.3

(a) Velocities   (b) Forces

Figure 2.2. *Blade Section forces and loads [1]*

2.1 Blade geometry design

A turbine operating at a variable speed can maintain the constant tip speed ratio (λ), who is defined by $\lambda = \Omega R / U_\infty$, required for the maximum power coefficient to be developed regardless of the wind speed. To develop the maximum possible power coefficient it's required suitable blade geometry; these conditions will now be derived.

The flow induction factors for optimal operation will be defined by:

$$a := \frac{1}{3} \text{ e } a' = \frac{a(1-a)}{\lambda^2 \mu^2}$$

2.4

To determinate the chord of the blade along the span,

$$\frac{N}{2\pi}\frac{c}{R}\lambda C_l = \frac{4\lambda^2\mu^2 a'}{\sqrt{(1-a)^2 + (a'\lambda\mu)^2}} \tag{2.5}$$

Where we define $\mu = {}^r/_R$, C_l as the lift coefficient and N as the number of blades.

Combining equations 2.4 and 2.6 we get,

$$c(\mu) = \frac{\frac{8}{9}}{\sqrt{\left(1-\frac{1}{3}\right)^2 + \lambda^2\mu^2\left(1 + \frac{2}{9(\lambda^2\mu^2)}\right)^2}}\frac{2\pi}{N}\frac{R}{C_l\lambda} \tag{2.6}$$

The local inflow angle ϕ at each blade station also varies along the blade span as shown in Equation 2.7 and Figure 2.4. This angle is defined by:

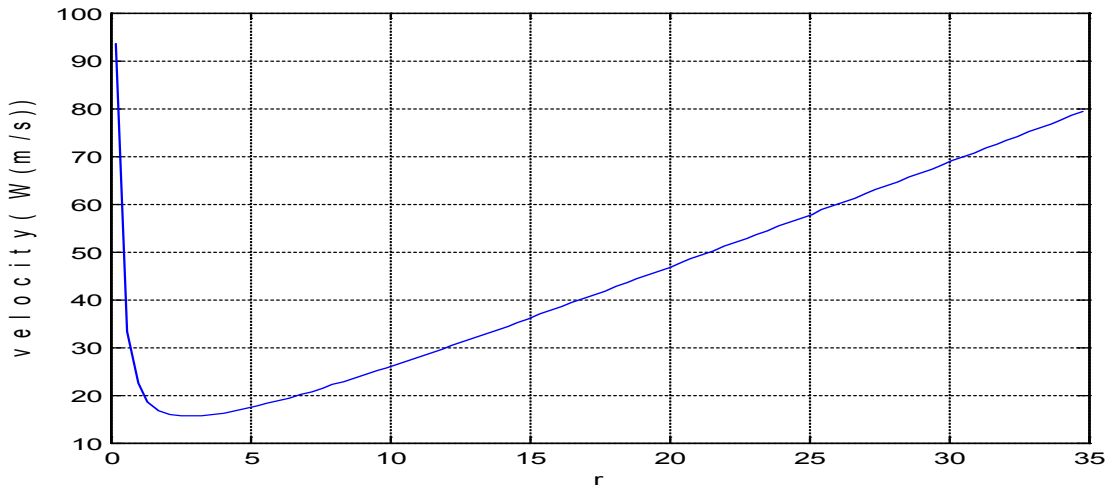$$tan\phi = \frac{(1-a)}{\lambda\mu(1+a')} \tag{2.7}$$

Figure 2.3. *Velocity variation along the span*

Close to the blade root the inflow angle is large which could cause the blade to stall in that region. If the lift coefficient is to be held constant such that drag is minimized everywhere then the angle of attack α also needs to be uniform at the appropriate value. For a prescribed angle of attack variation the design pitch angle ($\beta = \phi - \alpha$, in Figure 2.4 a (Optimal Twist Angle)) of the blade must vary accordingly.

2.2   A practical blade design

The blade design of Figure 2.4 b (Optimal Required Chord) is efficient but complex to build, and therefore costly. Suppose that the planform was prescribed to have a uniform taper such that the outer part of the blade corresponds closely to Figure 2.4 b (Practical Chord). A straight line drawn through the 70 percent and 90 percent span points as shown that figure not only simplifies the planform but removes a lot of material close to the root.

The expression for the new planform is,

$$\frac{c_u}{R} = \frac{8}{9\lambda 0.8}\left(2 - \frac{\lambda\mu}{0.8\lambda}\right)\frac{2\pi}{C_l\lambda N} \tag{2.8}$$

The 0.8 in equation 2.8 refers to the 80 percent point, midway between the target points.

Equations 2.6 and 2.8 can be combined to give the required span-wise variation of C_l for optimal operation.

$$C_l = \frac{8}{9} \frac{1}{\frac{Nc_u\lambda}{2\pi} \sqrt{\left(1 - \frac{1}{3}\right)^2 + \lambda^2\mu^2 \left[1 + \frac{2}{9(\lambda^2\mu^2)}\right]^2}}$$
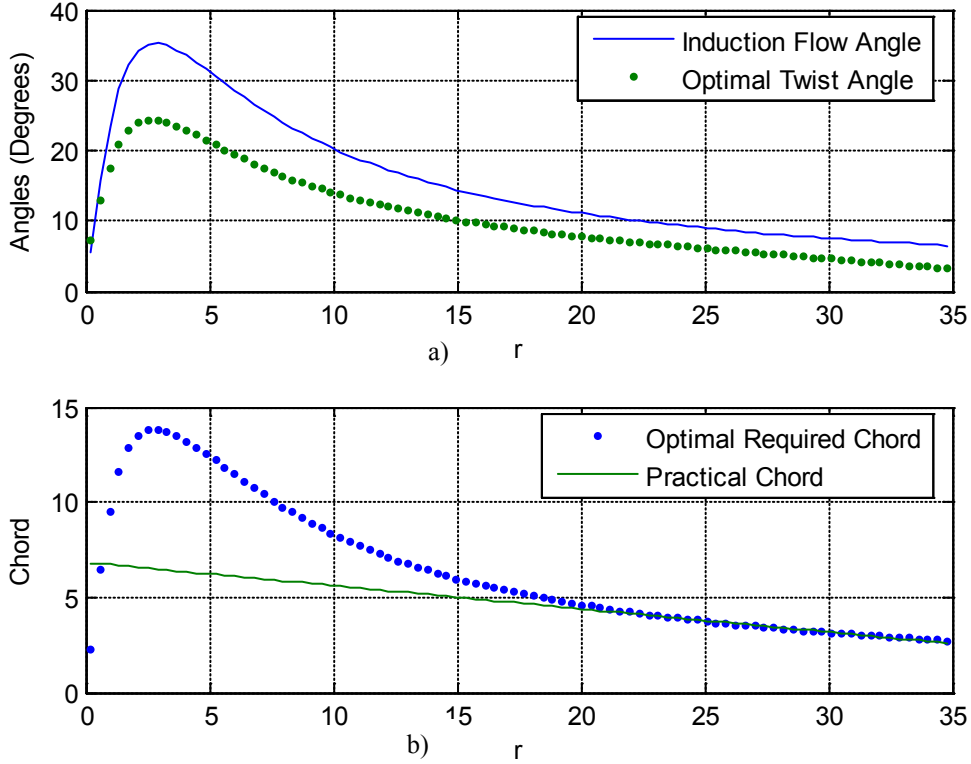
2.9

Figure 2.4. *Optimum Blade Design for Three Blades and λ = 6, a) Twist angle, b) Chord*

The lift coefficient can be written as a function of the angle of attack by the following way:

$$C_l = C_{l_\alpha}\alpha + C_{l_{\alpha_0}}$$

2.10

Therefore, the angle of attack can be written by:

$$\alpha = \frac{C_l - C_{l_{\alpha_0}}}{C_{l_\alpha}}$$

2.11

Where $C_{l_{\alpha_0}}$ is the lift coefficient at *zero* angle of attack, C_{l_α} is the slope of the C_l- α curve. All of these dates can be provided by simple two-dimensional airfoil parameters curve.

3 NUMERICAL EVALUATION USING THE DOUBLET LATICE METHOD

3.1 Numerical evaluation routine

To get a numerical solution for the potential flow problem, it's necessary to establish a work sequence defined by the follows steps:

- o **Selection of the singularity element.** It's the first and one of the most important decisions. The selection of the source, doublet or vortex representation and the method of discretizing these distributions will vary with the analyzed type of problem

- o **Grid and geometry discrezation.** Once the basic solution element is selected, the geometry of problem has to be subdivided to implement them. In this grid generating process, the elements' corner and collocation points are defined

- o **Influence coefficient.** In this phase, for each of this element, an algebraic equation is derived at the collocation point. To generate the coefficients in an automatic manner, a unit singularity strength is assumed and the element influence routine is called at each collocation points.

- o **Establish RHS.** The right-hand side of the matrix equation is the known portion of the free stream velocity and requires mainly the computation of geometrics quantities (e.g. $-Q_\infty \alpha$)

- o **Solve linear set of equations.** The set of equations is solved by standard matrix techniques. In this work, the Gaussian elimination is employed

- o **Secondary calculations: load, velocity, etc.** the solution of the matrix equation results in the singularity strengths providing the secondary calculations.

3.1.1 Selection of the singularity element

To define the panel, in this paper, we are going to make use of a quadrilateral geometry and the singularities will be taken as with constant intensity.

Quadrilateral source

Consider a surface element with a constant-strength source distribution σ per area bounded by four straight lines as describes in Figure 3.1. The element corner points are designated as, $(x_1, y_1, z_1), \dots, (x_4, y_4, z_4)$,
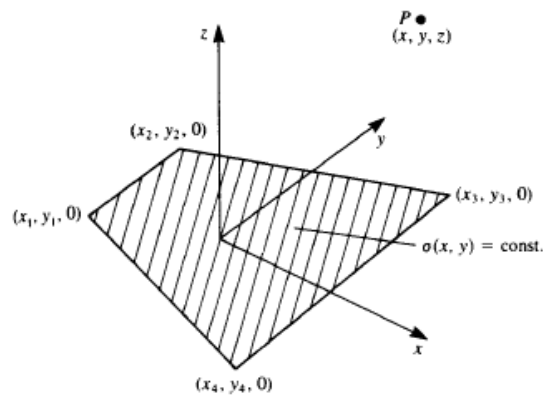

Figure 3.1. Quadrilateral constant strength source element [4]

The velocity components getting for this constant strength source distribution, based on the Hess & Smith results, will be,

$$u = \frac{\sigma}{4\pi}\left[\frac{(y_2 - y_1)}{d_{12}}\ln\frac{r_1 + r_2 - d_{12}}{r_1 + r_2 + d_{12}} + \frac{(y_3 - y_2)}{d_{23}}\ln\frac{r_2 + r_3 - d_{23}}{r_2 + r_3 + d_{23}} + \frac{(y_4 - y_3)}{d_{34}}\ln\frac{r_3 + r_4 - d_{34}}{r_3 + r_4 + d_{34}} \right. \tag{3.1}$$
$$\left. + \frac{(y_1 - y_4)}{d_{41}}\ln\frac{r_4 + r_1 - d_{41}}{r_4 + r_1 + d_{41}} \right]$$

$$v = \frac{\sigma}{4\pi}\left[\frac{(x_1 - x_2)}{d_{12}}\ln\frac{r_1 + r_2 - d_{12}}{r_1 + r_2 + d_{12}} + \frac{(x_2 - x_3)}{d_{23}}\ln\frac{r_2 + r_3 - d_{23}}{r_2 + r_3 + d_{23}} + \frac{(x_3 - x_4)}{d_{34}}\ln\frac{r_3 + r_4 - d_{34}}{r_3 + r_4 + d_{34}} \right. \tag{3.2}$$
$$\left. + \frac{(x_4 - x_1)}{d_{41}}\ln\frac{r_4 + r_1 - d_{41}}{r_4 + r_1 + d_{41}} \right]$$

$$w = \frac{\sigma}{4\pi}\left[\tan^{-1}\left(\frac{m_{12}e_1 - h_1}{zr_1}\right) - \tan^{-1}\left(\frac{m_{12}e_2 - h_2}{zr_2}\right) + \tan^{-1}\left(\frac{m_{23}e_2 - h_2}{zr_2}\right)\right.$$
$$- \tan^{-1}\left(\frac{m_{23}e_3 - h_3}{zr_3}\right) + \tan^{-1}\left(\frac{m_{34}e_3 - h_3}{zr_3}\right) - \tan^{-1}\left(\frac{m_{34}e_4 - h_4}{zr_4}\right)$$
$$\left.+ \tan^{-1}\left(\frac{m_{41}e_4 - h_4}{zr_4}\right) - \tan^{-1}\left(\frac{m_{41}e_1 - h_1}{zr_1}\right)\right]$$

3.3

Quadrilateral doublet

Consider a surface element with a constant-strength doublet distribution μ per area bounded by four straight lines as describes in Figure 3.2.
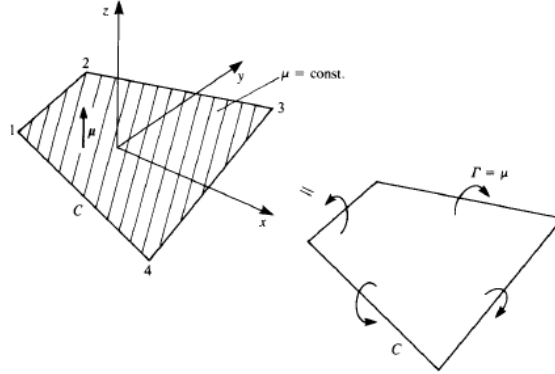

Figura 3.2. Quadrilateral constant strength doublet element and vortex ring equivalent [4].

Using the doublet element witch points in the z direction and following the Hess & Smith results, the velocity component will be,

$$u = \frac{\mu}{4\pi}\left[\frac{z(y_1 - y_2)(r_1 + r_2)}{r_1 r_2\{r_1 r_2 - [(x - x_1)(x - x_2) + (y - y_1)(y - y_2) + z^2]\}}\right.$$
$$+ \frac{z(y_2 - y_3)(r_2 + r_3)}{r_2 r_3\{r_2 r_3 - [(x - x_2)(x - x_3) + (y - y_2)(y - y_3) + z^2]\}}$$
$$+ \frac{z(y_3 - y_4)(r_3 + r_4)}{r_3 r_4\{r_3 r_4 - [(x - x_3)(x - x_4) + (y - y_3)(y - y_4) + z^2]\}}$$
$$\left.+ \frac{z(y_4 - y_1)(r_4 + r_1)}{r_4 r_1\{r_4 r_1 - [(x - x_4)(x - x_1) + (y - y_4)(y - y_1) + z^2]\}}\right]$$

3.4

$$v = \frac{\mu}{4\pi}\left[\frac{z(x_2 - x_1)(r_1 + r_2)}{r_1 r_2\{r_1 r_2 - [(x - x_1)(x - x_2) + (y - y_1)(y - y_2) + z^2]\}}\right.$$
$$+ \frac{z(x_3 - x_2)(r_2 + r_3)}{r_2 r_3\{r_2 r_3 - [(x - x_2)(x - x_3) + (y - y_2)(y - y_3) + z^2]\}}$$
$$+ \frac{z(x_4 - x_3)(r_3 + r_4)}{r_3 r_4\{r_3 r_4 - [(x - x_3)(x - x_4) + (y - y_3)(y - y_4) + z^2]\}}$$
$$\left.+ \frac{z(x_1 - x_4)(r_4 + r_1)}{r_4 r_1\{r_4 r_1 - [(x - x_4)(x - x_1) + (y - y_4)(y - y_1) + z^2]\}}\right]$$

3.5

$$w = \frac{\mu}{4\pi}\left[\frac{[(x - x_2)(y - y_1) - (x - x_1)(y - y_2)](r_1 + r_2)}{r_1 r_2\{r_1 r_2 - [(x - x_1)(x - x_2) + (y - y_1)(y - y_2) + z^2]\}}\right.$$
$$+ \frac{[(x - x_3)(y - y_2) - (x - x_2)(y - y_3)](r_2 + r_3)}{r_2 r_3\{r_2 r_3 - [(x - x_2)(x - x_3) + (y - y_2)(y - y_3) + z^2]\}}$$
$$+ \frac{[(x - x_4)(y - y_3) - (x - x_3)(y - y_4)](r_3 + r_4)}{r_3 r_4\{r_3 r_4 - [(x - x_3)(x - x_4) + (y - y_3)(y - y_4) + z^2]\}}$$
$$\left.+ \frac{[(x - x_1)(y - y_4) - (x - x_4)(y - y_1)](r_4 + r_1)}{r_4 r_1\{r_4 r_1 - [(x - x_4)(x - x_1) + (y - y_4)(y - y_1) + z^2]\}}\right]$$

3.6

3.1.2 Grid and geometry discretization

At this phase the surface is divided in N panels. N singularity elements will be placed at the center of each panel and the zero normal flow boundary condition will be imposed in it. Figure 3.3 shows the three-dimensional blade geometry discretization whit the collocation points.
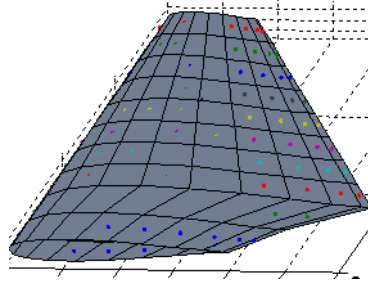

Figure 3.3. Discretization of the wind turbine blade geometry with the collocation points

3.1.3 Influence coefficients

The boundary conditions will be analyzed at this phase. Because it has not a unique solution of the problem, we must choose a source-doublet combination. The most frequently used resource is,

$$\sigma_k = \boldsymbol{n_k} \cdot \boldsymbol{Q}_\infty \qquad\qquad 3.7$$

Resulting in a unique set of equation with the doublet intensities as the only unknowns.

Wake panels will be expressed as trailing edge panels as show in Figure 3.4.
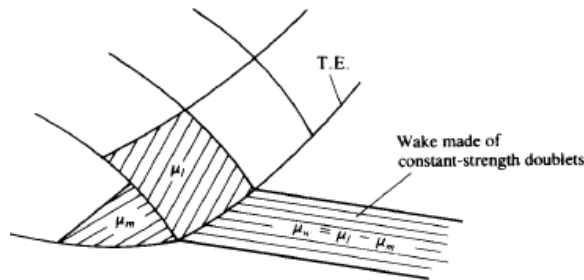

Figure 3.4 A typical wake panel shed by the trailing edge upper and lower panels [4]

The set of equation to solve has the following form,

$$
\begin{pmatrix}
a_{11} & a_{12} & \cdots & a_{1N} \\
a_{21} & a_{22} & & a_{2N} \\
\vdots & & \ddots & \vdots \\
a_{N1} & a_{N2} & \cdots & a_{NN}
\end{pmatrix}
\begin{pmatrix}
\mu_1 \\ \mu_2 \\ \vdots \\ \mu_N
\end{pmatrix}
= -
\begin{pmatrix}
b_{11} & b_{12} & \cdots & b_{1N} \\
b_{21} & b_{22} & & b_{2N} \\
\vdots & & \ddots & \vdots \\
b_{N1} & b_{N2} & \cdots & b_{NN}
\end{pmatrix}
\begin{pmatrix}
\sigma_1 \\ \sigma_2 \\ \vdots \\ \sigma_N
\end{pmatrix} \qquad 3.8
$$

3.1.4 Establish the RHS:

The main purpose of this work is to apply the panel method to a wind turbine blade to study its optimal performance. For that, we must take into account the blade rotation and, is in this point that we are going to include this effect. The way to simulate the rotation consists to set the free stream velocity around the surface. The parameters obtained in section **two** (eq. 2.1, 2.6 or 2.8, 2.7 and 2.11), will be the input to solve the RHS as shown in Figure 3.5.
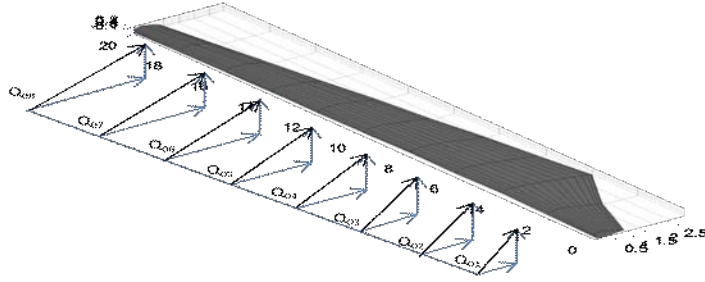
Figure 3.5. Free stream velocity varying along the span blade

Therefore the Right Hand Side of equation 3.8, describing the intensity source (eq. 3.7) by section will be,

$$\begin{pmatrix} RHS_1 \\ RHS_2 \\ \vdots \\ RHS_N \end{pmatrix} = - \begin{pmatrix} b_{11} & b_{12} & \cdots & b_{1N} \\ b_{21} & b_{22} & & b_{2N} \\ \vdots & & \ddots & \vdots \\ b_{N1} & b_{N2} & \cdots & b_{NN} \end{pmatrix} \begin{pmatrix} n_{x1} \cdot Q_{x1} + n_{y1} \cdot Q_{y1} + n_{z1} \cdot Q_{z1} \\ n_{x2} \cdot Q_{x2} + n_{y2} \cdot Q_{y2} + n_{z2} \cdot Q_{z2} \\ \vdots \\ n_{xN} \cdot Q_{xN} + n_{yN} \cdot Q_{yN} + n_{zN} \cdot Q_{zN} \end{pmatrix}$$ 3.9

3.1.5   Solution of linear equations

The system is ready to be solved by implementation of the Gaussian elimination. The equations 3.8 and 3.9 give,

$$\begin{pmatrix} \mu_1 \\ \mu_2 \\ \vdots \\ \mu_N \end{pmatrix} = \begin{pmatrix} a_{11} & a_{12} & \cdots & a_{1N} \\ a_{21} & a_{22} & & a_{2N} \\ \vdots & & \ddots & \vdots \\ a_{N1} & a_{N2} & \cdots & a_{NN} \end{pmatrix}^{-1} \begin{pmatrix} RHS_1 \\ RHS_2 \\ \vdots \\ RHS_N \end{pmatrix}$$ 3.10

3.1.6   Secondary calculations

One of the most important advantages of the potential flow formulation is that the computation of the surface velocity components and pressures is determinable by the local properties of the solution. These perturbation velocity components on the surface panel can be obtained by:

$$q_l = \frac{1}{2\Delta l}(\mu_{l+1} - \mu_{l-1}) \qquad q_m = \frac{1}{2\Delta m}(\mu_{m+1} - \mu_{m-1}) \qquad q_n = \sigma_n$$ 3.11

Where q_l, q_m and q_n are the velocity component in the longitudinal (x direction), transversal (y direction) and normal direction (z direction) and they are already differentiated by the central differences method. Δl and Δm are the panel length in those direction (Figure 3.6).
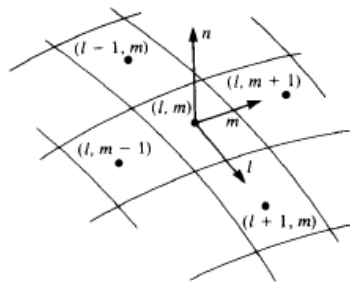

Figure 3.6. Nomenclature used for the differentiation of the velocity potential for local tangential velocity calculations [4]

The total velocity for each panel will be,

$$v_i = \sqrt{q_{l_i}{}^2 + q_{m_i}{}^2 + q_{n_i}{}^2}$$ 3.12

The pressure coefficients for each rotational blade panel will be thinking by the following form,

$$Cp_i = 1 - \frac{v_i^2}{Q_{\infty_i}^2}$$

3.13

Note that for this equation, the free stream velocity Q_{∞_i}, vary for each section along the span (see Figure 3.5).

The **i-th** panel contribution for aerodynamic loads components, ΔF_k, will be,

$$\Delta F_{k_i} = -Cp_i \left(\frac{1}{2}\rho Q_{\infty_i}^2\right)\Delta S_i n_{k_i}$$

3.14

Note that the **i** subscript represents the analyzed panel while the **k** subscript represent the direction (*l, m, n*) of the force component. The sum of the panels' contribution to the total force is done by the following form; first we have to sum the **i** panels' contribution of the same section (Figure 3.7).

$$F_j = \sum_{i=1}^{N} \Delta F_i \Big|_{seção\ j}$$

3.15

Where F_j is the Total force vector of **j** section.

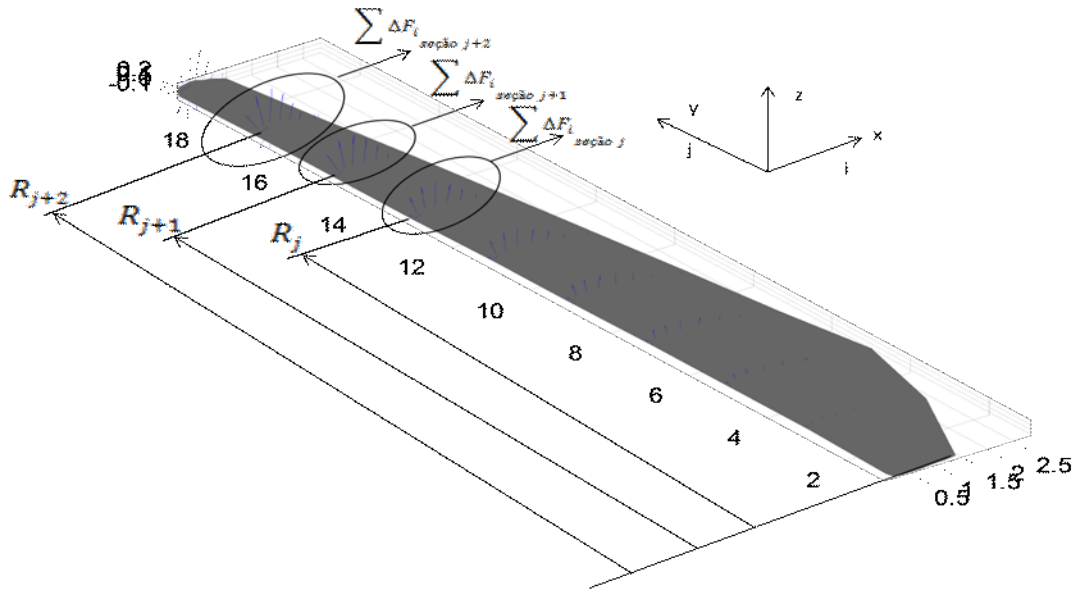***Figure 3.7. Sum by section of the forces contributions necessaries to find the torque***
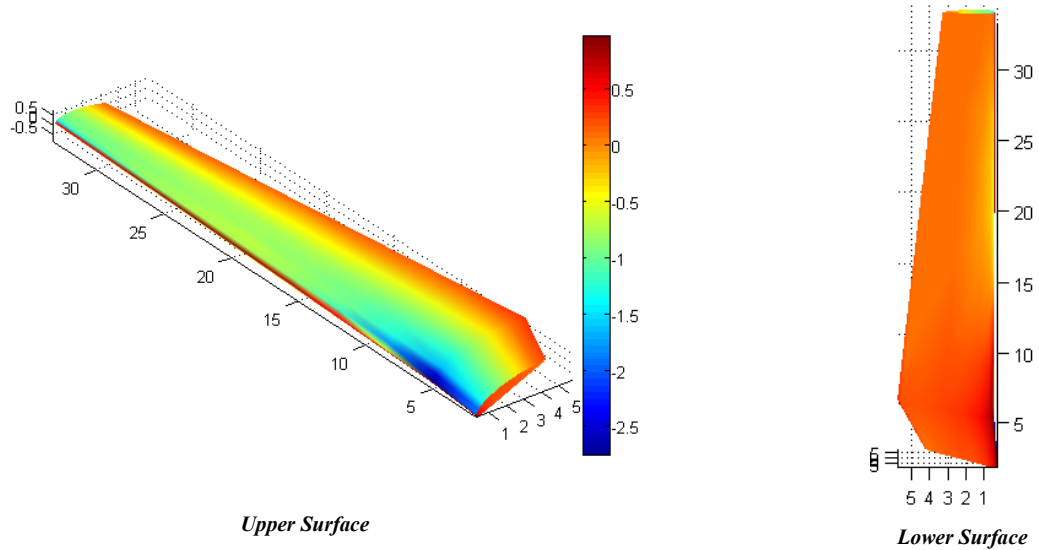
The torque developed for each **j** section can be expressed by the cross product between the vector blade radio and the force vector.

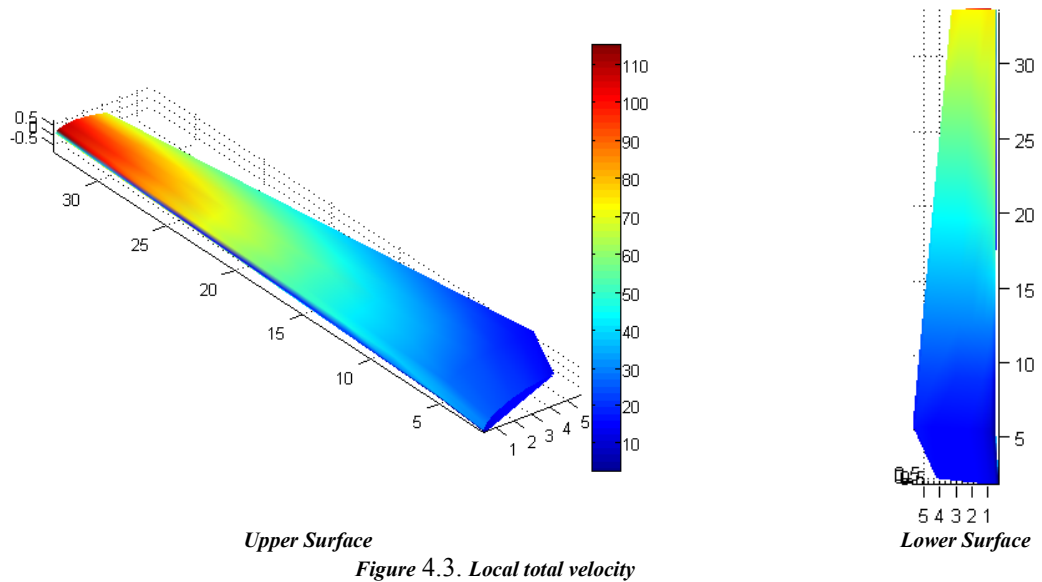$$T_j = \begin{bmatrix} i & j & k \\ 0 & R_j & 0 \\ F_{x_j} & F_{y_j} & F_{z_j} \end{bmatrix}$$

3.16

The total torque will be the sum of all **j** torques,
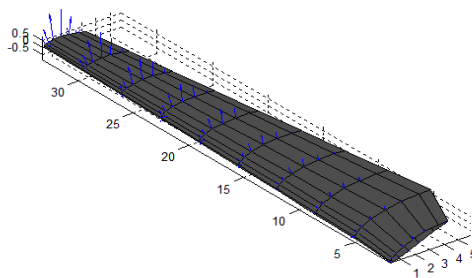
$$T = \sum_{j=1}^{N} \Delta T_j$$

3.17

The Power (P) can be written as the torque generated by the blade and the rotational velocity (ω). Considerer that ω will be act in z direction only.

$$P = \left(T_x, T_y, T_z\right) \cdot (0,0,\omega) \qquad\qquad 3.18$$

The power coefficient (C_{Pot}) that represent the blade power extraction and the power offered by the wind, can be written as,

$$C_{Pot} = \frac{P}{\frac{1}{2}\rho U_\infty{}^3 \pi R^2} \qquad\qquad 3.19$$

4   NUMERICAL SIMULATIONS

The theory presented in the previous sections was used to predict the aerodynamic performance of a 2 MW wind turbine and the firsts result of this simulation were gotten in section two (Figure 2.4 and Figure 2.3). The total free stream rotational velocity $W(r)$ (then called Q_∞), the induction flow angle, the optimal twist angle and the required chord are going to be the input data to the numerical panels method

The wind turbine program part has been thought to have three blades equally spaced along the circumferential direction, but the blade simulation program part has only one blade to be calculated. This is one of the limitations of the program for now. Although we are going to get only the power of one blade, the results are very encouraging to keep working.

For the present work, the aerodynamic characteristic curves in terms of lift coefficient versus angle of attack and drag coefficient versus angle of attack of a NACA 4412 airfoil was taken into account. The adopted criterion for choosing the best airfoil for the wind turbine blade is based on how much aerodynamic power the airfoil can effectively generate and transfer to the wind turbine shaft for a given operating condition.

This procedure obviously requires an iterative process. Figure 4.1 shows a typical blade geometry obtained using the procedure described in section two (Figure 2.4).

Figure 4.1. *Blade Geometry (Practical Chord)*

The pressure coefficients of the blade take into account that the free stream Q_∞ is now variable along the span, as shown in Figure 4.2.

Upper Surface

Lower Surface

Figure 4.2. *Pressure Coeficients*

The total local velocity for each panel is represented in Figure 4.3.

Upper Surface

Lower Surface

Figure 4.3. *Local total velocity*

The local forces are placed at the collocation points. The program uses the collocation points to create the geometry and places the forces on them as shown in Figure 4.4.

Figure 4.4. *Local forces*

For this case, the calculated power coefficient for one blade will be,

$$C_{Pot} = \frac{P}{q Q_\infty \pi R^2} = 0.105$$

And for this single blade configuration, the development power will be: $P = 0.6\ MW$ for $\lambda = 5.8$.

A very important parameter in wind turbine design is the C_{Pot} vs. λ curve. This program is enables to find this curve and, for this case, the results are shown in Figure 4.5. Note that in this figure the maximum power coefficient is found at $\lambda = 5$. This means that one more iteration has to be done.

We have the possibility to work with the 'Optimal required Chord' from Figure 2.4 giving the blade geometry presented in Figure 4.6. For this case the power coefficient obtained is $C_{Pot} = 0.12$ and the power is $P = 0.7\ MW$. The difference from the previous case is not significant in respect to the power, so it's not worth adding material at the root.
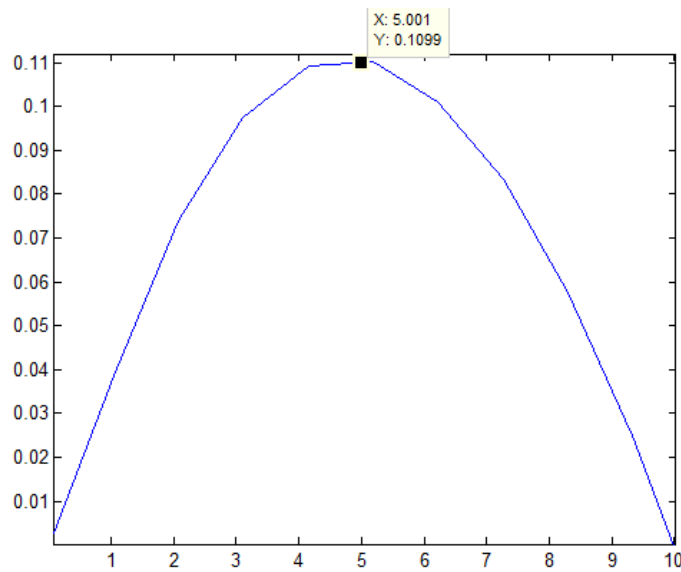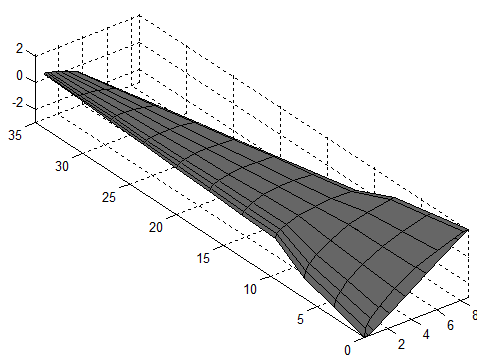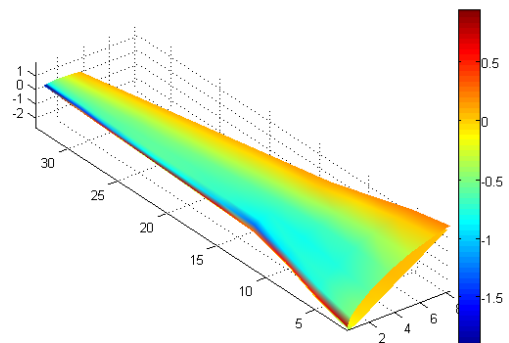

Figure 4.5. *Power coefficient (C_{Pot}) vs. relação de velocidade de ponta (λ)*

Blade geometry   **Power coefficient.**

Figure 4.6. *Optimal required chord blade design*

5   CONCLUSIONS

A consistent aerodynamic model for wind turbines with variable geometry was presented and discussed in this work. Details about the numerical implementation were also presented and discussed. The proposed formulation is based on the Glauert Blade Element Theory to get the input data like resultant relative velocity, required optimal and practical chord, inflow and twist angles, etc. Three-dimensional doublet lattice method was applied to calculate power and others important blade parameters. This work does not take into account tip and rotational wake losses yet. Because the doublet lattice method is based in potential flow theory, there is not turbulent and detachment flow effects, but it includes the total tridimensional pressure coefficient which indicates possible detachment points or turbulence origins. That means we can design the blade to avoid these effects.

A study case in terms of aerodynamic performance was presented for a 2 MW wind turbine. The first program part (section two) enables the calculation of design parameters for three blades, but the second one can only calculate aerodynamics parameters for one blade.

The results have proven to be very consistent but have not been validated yet. This will be done soon with a commercial computational fluid-dynamics programs package.

The potential flow formulation has some advantages and disadvantages with relation to the finite element method. Between the advantages, the most importants are the computational velocity and the inter-relationship that can be achieved with structural packages, which is what we are looking for.

6   ACKNOWLEDGEMENTS

7   REFERENCES

[1] Burton, T., 2001, "Wind Energy Handbook", Ed. John Wiley and Sons Ltd., Chichester, New York, 624 p.

[2] Donadon, M. V., Savanov, R., Menezes, J. C., Moreira Filho, L. A., "A Numerical Tool to Design Blades for horizontal Axis Wind Turbines with Variable Geometry" V National Congress of Mechanical Engineering, CONEM 2008, Salvador, Bahia, Brazil.

[3] Menezes, J.C., Donadon, M.V., 2009, "Optimum Blade Design of a 2 MW Horizontal Axis Wind Turbine", 20th International Congress of Mechanical Engineering, Gramado, RS, Brazil.

[4] Katz and Plotkin, 2001, "Low Speed Aerodynamics", second edition, Cambridge University Press, New York, 2001.

8   RESPONSIBILITY NOTICE

The authors are the only responsible for the printed material included in this paper